Annals of Diagnostic Pathology 44 (2020) 151434

Contents lists available at ScienceDirect

Annals of Diagnostic Pathology

journal homepage: www.elsevier.com/locate/anndiagpath

Original Contribution

Kaposiform hemangioendothelioma and tufted angioma – (*epi*)genetic analysis including genome-wide methylation profiling☆

Roel W. Ten Broek[a], Christian Koelsche[b], Astrid Eijkelenboom[a], Thomas Mentzel[c], David Creytens[d], Christian Vokuhl[e], Joost M. van Gorp[f], Yvonne M. Versleijen-Jonkers[g], Carine J. van der Vleuten[h], Patrick Kemmeren[i], Ellen van de Geer[i], Andreas von Deimling[j,k], Uta Flucke[a,i,*]

[a] Department of Pathology, Radboud University Medical Center, Nijmegen, the Netherlands
[b] Department of General Pathology, University of Heidelberg, Heidelberg, Germany
[c] Dermatopathology Bodensee, Friedrichshafen, Germany
[d] Department of Pathology, Ghent University Hospital, Ghent, Belgium
[e] Department of Pediatric Pathology, University Hospital of Schleswig-Holstein, Kiel, Germany
[f] Department of Pathology, St Antonius Hospital, Nieuwegein, the Netherlands
[g] Department of Medical Oncology, Radboud University Medical Center, Nijmegen, the Netherlands
[h] Department of Dermatology, Radboud University Medical Center, Nijmegen, the Netherlands
[i] Princess Màxima Center for Pediatric Oncology, Utrecht, the Netherlands
[j] Department of Neuropathology, University of Heidelberg, Heidelberg, Germany
[k] CCU Neuropathology, German Cancer Center, Heidelberg, Germany

ARTICLE INFO

Keywords:
Kaposiform hemangioendothelioma
Tufted angioma
Vascular malformations
Genetics
Epigenetics
Methylation profiling

ABSTRACT

Kaposiform hemangioendothelioma (KHE) is a locally aggressive vascular condition of childhood and is clinicopathologically related to tufted angioma (TA), a benign skin lesion.

Due to their rarity molecular data are scarce.

We investigated 7 KHE and 3 TA by comprehensive mutational analysis and genome-wide methylation profiling and compared the clustering, also with vascular malformations.

Lesions were from 7 females and 3 males. The age range was 2 months to 9 years with a median of 10 months. KHEs arose in the soft tissue of the thigh (n = 2), retroperitoneum (n = 1), thoracal/abdominal (n = 1), supraclavicular (n = 1) and neck (n = 1). One patient presented with multiple lesions without further information. Two patients developed a Kasabach-Merritt phenomenon. TAs originated in the skin of the shoulder (n = 2) and nose/forehead (n = 1).

Of the 5 KHEs and 2 TAs investigated by DNA sequencing, one TA showed a hot spot mutation in *NRAS*, and one KHE a mutation in *RAD50*.

Unsupervised hierarchical clustering analysis indicated a common methylation pattern of KHEs and TAs, which separated from the homogeneous methylation pattern of vascular malformations.

In conclusion, methylation profiling provides further evidence for KHEs and TAs potentially forming a spectrum of one entity. Using next generation sequencing, heterogeneous mutations were found in a subset of cases (2/7) without the presence of *GNA14* mutations, previously reported in KHE and TA.

Original Contribution

1. Introduction

The term kaposiform hemangioendothelioma (KHE) was introduced by Zukerberg et al. in 1993 for a vascular tumor with locally aggressive behavior and morphological features similar to Kaposi sarcoma [1]. These lesions mainly occur in (early) childhood but also have been infrequently reported in (young) adults. Tumors may arise in superficially or deep soft tissue and are mainly located in the extremities.

☆ This research did not receive any specific grant from funding agencies in the public, commercial, or not-for-profit sectors.
* Corresponding author at: Radboud University Medical Center, Department of Pathology, P.O. Box 9101, 6500 HB Nijmegen, the Netherlands.
E-mail address: uta.flucke@radboudumc.nl (U. Flucke).

https://doi.org/10.1016/j.anndiagpath.2019.151434

1092-9134/ © 2019 The Author(s). Published by Elsevier Inc. This is an open access article under the CC BY-NC-ND license (http://creativecommons.org/licenses/BY-NC-ND/4.0/).

Other localizations are the trunk, retroperitoneum, head and neck, mediastinum and visceral organs as thymus and spleen [1,2]. Kasabach-Merritt-phenomenon or disseminated intravascular coagulation with thrombopenia and anemia are adverse clinical conditions often associated with a deep anatomic site [1-8].

One of the intriguing morphological features previously described is the presence of large lymphatic vessels, called lymphangiomatosis showing resemblance to vascular malformations [1,2,4,5]. Therefore, it seemed worthwhile to investigate, whether there is a possible link with vascular malformations.

Tufted angioma (TA) is discussed to be the dermal counterpart of KHE with a benign clinical course due to the superficial origin [2,4,5-7].

From the recent clinical point of view, treatment with sirolimus has been shown successful in KHE and therefore a biopsy for diagnostic purposes would influence treatment decisions. However clinical and morphological diagnosis can be challenging and diagnostically supportive molecular data are not established [2,8].

We analyzed FFPE material from KHE cases ($n = 7$) and tufted angiomas ($n = 3$) using comprehensive mutational analysis and genome-wide methylation profiling and compared the data with those of vascular malformations ($n = 14$).

2. Material and methods

The cases were retrieved from the authors' (referral) files using the WHO criteria [9]. Clinical details were obtained from the referring physicians. The study was conducted in accordance with the Code of Conduct of the Federation of Medical Scientific Societies of Germany and the Netherlands.

In all cases the tissue was fixed in 4% buffered formalin, routinely processed and embedded in paraffin; 2–4 μm thick sections were stained with hematoxylin and eosin.

Immunohistochemistry was performed using standard procedures and the following primary antibodies, ERG (EPR3864, 1:2000, ABCam, Cambridge, UK), CD31 (JC70 A, 1:100, DAKO, Glostrup, Denmark), CD34 (My10, 1:100, BD Biosciences, Heidelberg, Germany), D2–40 (D2–40, 1:100, DAKO, Glostrup, Denmark), GLUT1 (SPM498, 1:400, Zytomed Systems, Berlin, Germany), WT1 (6F–H2, 1:400, DAKO, Glostrup Denmark)

2.1. DNA isolation, genome-wide DNA methylation data generation and pre-processing

Representative tumor tissue with highest available tumor content was chosen for DNA extraction. The Maxwell® 16 FFPE Plus LEV DNA Kit or the Maxwell® 16 Tissue DNA Purification Kit (for frozen tissue) was applied on the automated Maxwell device (Promega, Madison, WI, USA) according to the manufacturer's instructions. All tumors had a total amount of > 100 ng DNA and were suitable for the array-based DNA methylation analysis. All tumors were subjected to Illumina Infinium HumanMethylation450 (450 k) BeadChip or the successor EPIC/850 k BeadChip (Illumina, San Diego, USA) analysis at the Genomics and Proteomics Core Facility of the German Cancer Research Center (DKFZ) Heidelberg. DNA methylation data were normalized by performing background correction and dye bias correction (shifting of negative control probe mean intensity to zero and scaling of normalization control probe mean intensity to 20,000, respectively). Probes targeting sex chromosomes, probes containing multiple single nucleotide polymorphisms and those that could not be uniquely mapped were removed. Probes from the EPIC array were excluded if the predecessor Illumina Infinium 450 k BeadChip did not cover them, thereby making data generated by both 450 k and EPIC feasible for subsequent analyses. In total, 438,370 probes were kept for analysis.

Table 1
Diagnoses and clinical features.

#	Diagnosis	Sex/age	Site and clinical features	Follow-up
1	KHE	m/8 mo	Intrathoracal/intraabdominal	NA
2	KHE	m/6 mo	NA, multiple lesions	NA
3	KHE	f/5 mo	Supraclavicular, KMP	NA
4	KHE	m/2 mo	Neck, intramuscular	NA
5	KHE	f/12 mo	Thigh, deep	NA
6	KHE	f/4 mo	Thigh, skin, soft tissue, inoperable	NA
7	KHE	f/15 mo	Retroperitoneum, KMP	DOD, 1 mo
8	TH	f/15 mo	Shoulder	CE
9	TH	f/18 mo	Shoulder, multiple lesions	CE
10	TH	f/9 y	Nose/forehead	NA

KHE, kaposiform hemangioendothelioma; TA, tufted angioma; m, male; f, female; mo, months; y, years; KMP, Kasabach-Merritt phenomenon; NA, not analyzed; CE, complete excision; DOD, dead of disease.

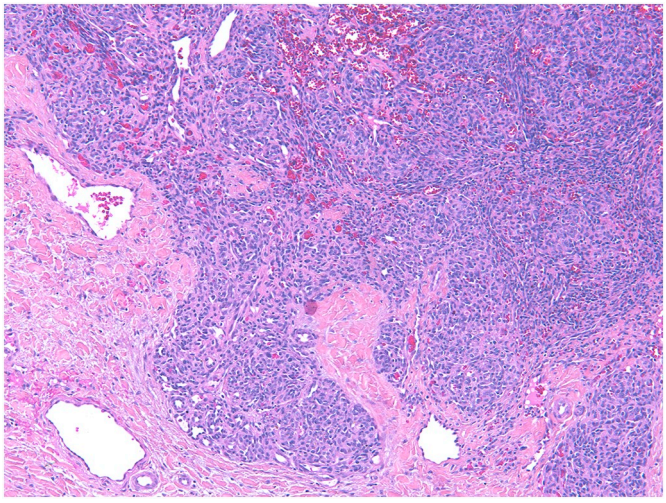

Fig. 1. KHE, consisting of vasoformative plump spindle cells with monomorphic elongated nuclei arranged in coalescing nodules. Note the larger vascular malformation-like vessels in the surrounding (Case 1).

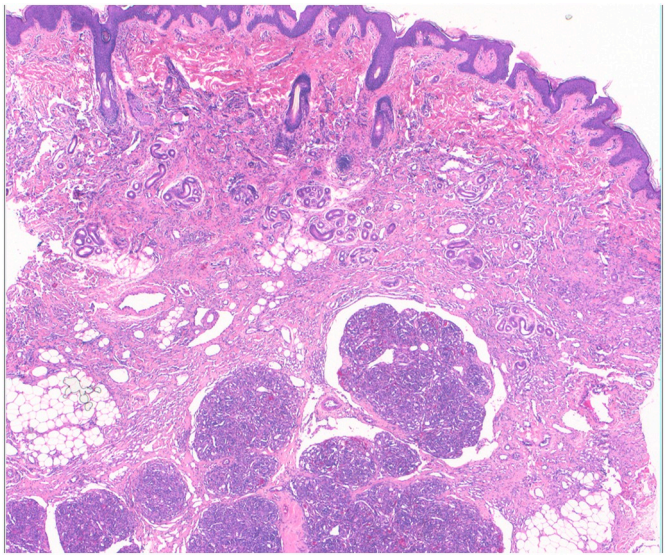

Fig. 2. TA showing the typical “cannonball structures” and diffuse growing subtle vascular channels (Case 8).

Table 2
Identified mutations.

#	Diagnosis	Mutation
1	KHE	No mutation
2	KHE	No mutation
3	KHE	Not analyzed
4	KHE	No mutation
5	KHE	No mutation
6	KHE	Not analyzed
7	KHE	*RAD50*, R1185X
8	TA	*NRAS*, Q61H
9	TA	Not analyzed
10	TA	No mutation

2.2. Unsupervised clustering, t-SNE analysis and cumulative copy number plotting

For unsupervised hierarchical clustering, we selected 10,000 probes that showed the highest median absolute deviation (MAD) across the beta values. Samples were hierarchically clustered using the Euclidean distance and Ward's linkage method. Hierarchical clustering using Euclidean distance and complete linkage reordered methylation probes. The unscaled methylation levels were shown in a heat map from unmethylated state (blue color) to methylated state (red color). For unsupervised 2D representation of pairwise sample correlations, dimensionality reduction by t distributed stochastic neighbor embedding (t-SNE) was performed using the 10,000 most variable probes, a perplexity of 20 and 2500 iterations. Novel methylation groups were tested

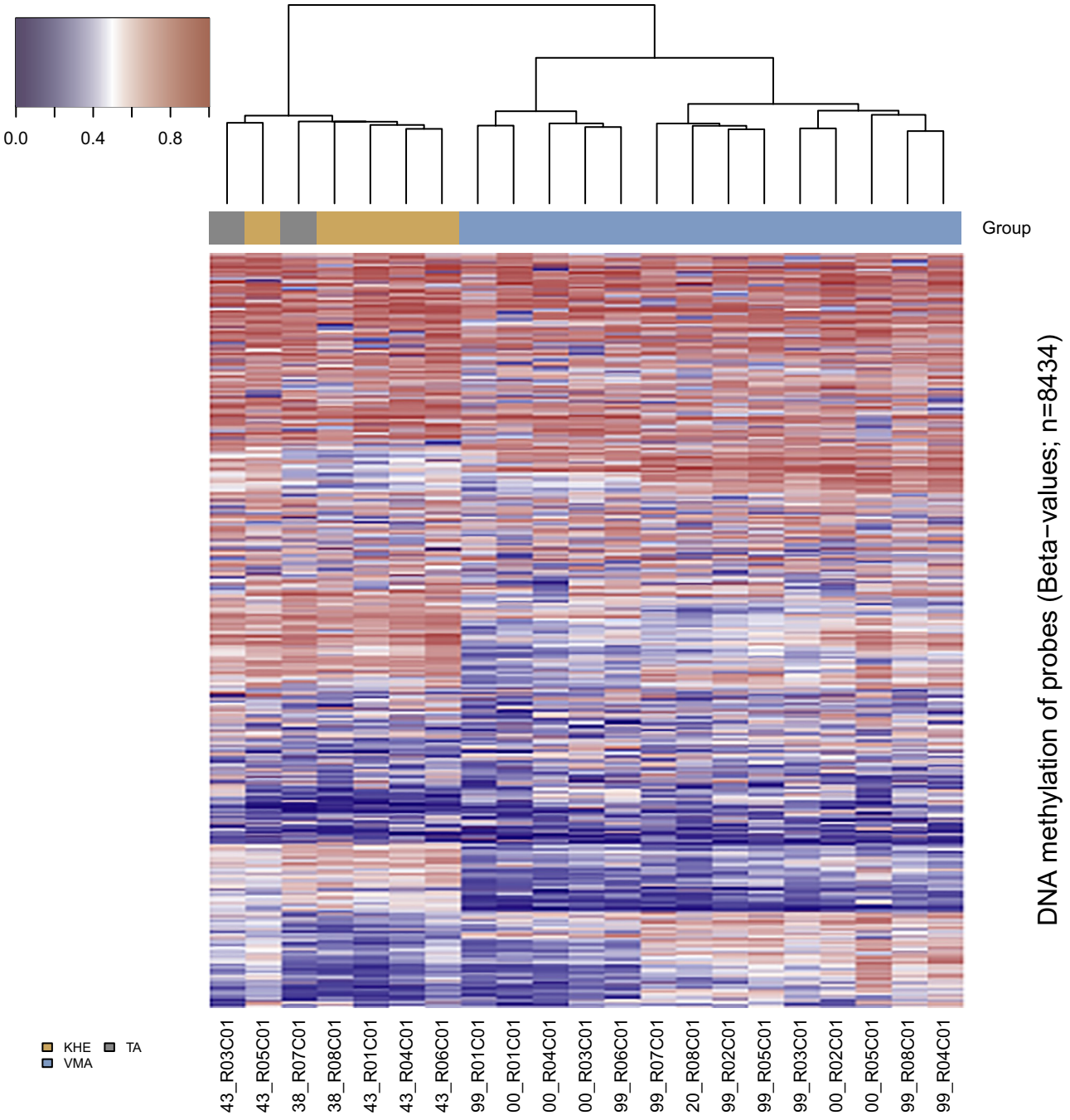

Fig. 3. Unsupervised hierarchical clustering of methylation shows a similar profile of TA and KHE demonstrating that these lesions are epigenetically related in contrast to vascular malformations, which cluster apart.

Table 3
Histological, clinical and molecular features of the included vascular malformations.

#	Sex/age (y)	Site	Clinical features	Histology	Mutations
1	m/53	Dura	Atypical vascular lesion	Capillary malformation	*GNAQ*: c.627A > C (p.(Gln209His)) and *PIK3CA*: c.3140A > G (p.(His1047Arg))
2	f/45	Arm	KTS spectrum with port wine stain	Venous malformation	*KRAS*: c.436G > A (p.(Ala146Thr))
3	f/81	Lower lip	port wine stain in SWS	Combined malformation	*GNAQ*: c.548G > A (p.(Arg183Gln))
4	m/76	Lower leg	AVM with ulceration	AVM	*KRAS*: c.34G > T (p.(Gly12Cys))
5	f/70	Buttock subcutis	unknown	Veno-capillary malformation	*KRAS*: c.35G > A (p.(Gly12Asp))
6	m/15	Skin (clavicula)	non congenital high flow lesion	Veno-capillary malformation	*GNAQ*: c.626A > T (p.(Gln209Leu))
7	m/41	Flank	lipoma-like lesion	Venous malformation	*KRAS*: c.35G > C (p.(Gly12Ala))
8	f/56	Flank	vascularized tumor	Veno-capillary malformation	*KRAS*: c.35_38delinsCTCA (p.(Gly12_Gly13delinsAlaHis))
9	f/20	Muscle	Unknown	Combined vascular malformation	not identified
10	f/64	Epidural	Epidural mass	Veno-capillary malformation	*GNAQ*: c.627A > C (p.(Gln209His))
11	f/43	Upper lip	KTS spectrum with port wine stain;	Venous malformation	*GNAQ*: c.548G > A (p.(Arg183Gln))
12	m/12	Skin (thorax)	multiple eruptive vascular lesions	Capillary malformation	*NRAS*: c.182A > G (p.(Gln61Arg))
13	m/32	Cheek	KTS spectrum with lymphedema	Venous malformation	*KRAS*: c.64C > A (p.(Gln22Lys))
14	f/10	Foot, bladder wall	KTS/PROS	Combined vascular malformation	*PIK3CA*: c.1633G > A (p.(Glu545Lys))

M, male; f, female; KTS, Klippel-Trenauney Syndrome, PROS, PIK3CA-related overgrowth spectrum.

for stability by varying the number of the most variable probes.

2.3. Next generation DNA sequencing

Next generation DNA sequencing was performed as described by Sahm et al. 2016 and ten Broek et al. 2019 [10,11].

3. Results

KHEs (n = 7) and TAs (n = 3) were from seven females and three males. The age range was 2 months to 9 years with a median of 10 months. KHEs arose in the thigh (n = 2), retroperitoneum (n = 1), thoracal/abdominal (n = 1), supraclavicular (n = 1) and neck (n = 1). One patient presented with multiple lesions but there was no information about their sites. Patients #3 and 7 developed a Kasabach-Merritt phenomenon. The lesions diagnosed as TA originated in the skin of the shoulder (n = 2) and nose/forehead (n = 1). One of the TAs of the shoulder was multifocal (Table 1).

Histomorphologically, KHEs showed infiltrative growing irregular nodules surrounded by desmoplastic stroma. The nodules consisted of vasoformative spindle cells with variable convoluting and slit-like small lumina. Sometimes lumina were very subtle. The endothelial cells possessed monomorphic enlongated and tapered nuclei (Fig. 1). Small areas depicted a more epithelioid aspect. Lymphatics in variable sizes were scattered throughout. The TAs showed prominent cannonball structures accompanied by lymphatic vessels in the surrounding. In one case also a diffuse growing spindle cell component was obvious (Fig. 2). The nuclei were not different from KHE cases.

Using immunohistochemistry, all analyzed lesions were positive for CD31 (9/9), CD34 (7/7) and ERG (1/1). Patchy positivity of D2–40 was seen in 6/6 KHEs and in one tested TA. In two KHEs GLUT1 was focally expressed and in one investigated KHE case, WT1 was partly absent.

Data of the comprehensive mutational analysis were shown in Table 2.

One TA harbored a mutation in *NRAS* (p.Q61H) and one KHE a stopgain mutation in *RAD50* (pR1185X).

3.1. Genome-wide methylation analysis

KHEs (n = 5) and TAs (n = 2) formed a homogeneous methylation cluster both by unsupervised hierarchical clustering and by t-SNE analysis, which kept stable when varying the number of CpGs (Fig. 3).

Fourteen vascular malformations formed a separate cluster (Fig. 3). Their clinical, histopathological and molecular data are depicted in Table 3.

4. Discussion

The molecular understanding of vascular neoplasms is steadily growing. However KHE and TA are poorly understood. To the best of our knowledge, we here present for the first time epigenetic data on these rare tumors and provide further evidence that KHE and TA share a common origin without a relationship to vascular malformation.

A genetic based study has found *GNA14* mutations in KHE and TA [12]. However, these mutations are not entity specific since they are also described in other vascular lesions like lobular capillary hemangioma, congenital hemangioma, anastomosing hemangioma and hepatic small vessel neoplasm [12-14], which are potential differential diagnoses [2].

In our series (n = 7) we were not able to find *GNA14* mutations. Instead, comprehensive mutational analysis showed a mutation in *NRAS* in one TA, and *RAD50* in one KHE.

The proto-oncogen *NRAS* encodes a small GTPase regulating cell proliferation. Mutations in *NRAS* stimulate the RAS-RAF-MEK-ERK signaling pathway and were also identified in vascular malformations [11]. Recently, recurrent *NRAS* hot spot mutations have been reported in kaposiform lymphangiomatosis (KLA) [[15]]. One could argue that KLA and KHE are related lesions and indeed there are overlapping clinicopathological features, including Kasabach-Merritt phenomenon. However, in contrast to a local process of KHE in most of the cases, KLAs are reported often as multifocal lesions with involvement of the thoracic cavity, retroperitoneum, bone, spleen and soft tissue. Morphologically, both lesions show spindled endothelial cells and abnormal lymphatic channels. It seems that the spindle cell component of KLA is frequently arranged in parallel fashion, poorly marginated clusters and anastomosing strands/sheets, whereas KHEs grow in confluent nodules with glomeruloid features. Overall, similarities of these entities are remarkable [16].

Our *NRAS* mutated case was a tufted hemangioma with typical cannonball structures and a diffuse growing component consisting of spindled endothelial cells suggesting that KHE, KLA and TA are related.

RAD50, mutated in one of the KHE cases of our series, belongs to the ABC transporter family of ATPases and is normally involved in DNA double-strand break repair, cell cycle checkpoint activation, telomerase maintenance, and meiotic recombination. Mouse knockout studies suggest an essential role in growth and viability [17-19].

The epigenetic genome-wide methylation profile showed similarities between tufted angioma and KHE congruent with the morphological features supporting that these lesions are strongly related. However, this group is clustered apart from vascular malformations demonstrating that there may be no relationship despite overlapping mutations and the presence of abnormal lymphatic channels in KHE

and TA. Of note, similar treatment effect of sirolimus in KHE and vascular malformations has been reported, possibly implying that overlapping pathways are activated [20-22].

In conclusion, the largely similar epigenetic profiles of KHE and TA confirm that these lesions are related clustering apart from vascular malformations. However, the genetic features of KHE and TA seem to be heterogeneous and need to be further explored. Whether KHE and KLA are a spectrum of one entity will be another object of investigation.

Declaration of competing interest

There are no conflicts of interest.

References

[1] Zukerberg LR, Nickoloff BJ, Weiss SW. Kaposiform hemangioendothelioma of infancy and childhood. An aggressive neoplasm associated with Kasabach-Merritt syndrome and lymphangiomatosis. Am J Surg Pathol 1993;17:321–8.

[2] Putra J, Gupta A. Kaposiform haemangioendothelioma: a review with emphasis on histological differential diagnosis. Pathology 2017;49:356–62.

[3] Enroljas O, Wassef M, Mazoyer E, Frieden IJ, RieuPN, Drouet L, Taïeb a, Stalder JF, Escande JP. Infants with Kasabach-Merritt syndrome do not have “true”hemangiomas. J Pediatr 1997;130:631–640.

[4] Lyons LL, North PE, Mac-Moune Lai F, Stoler MH, Folpe AL, Weiss SW. Kaposiform hemangioendothelioma: a study of 33 cases emphasizing its pathologic, immunophenotypic, and biologic uniqueness from juvenile hemangioma. Am J Surg Pathol 2004;28:559–68.

[5] North PE. Pediatric vascular tumors and malformations. Surg Pathol 2010;3:455–94.

[6] Wassef M, Blei F, Adams D, Alomari A, Baselga E, Berenstein A, et al. On behalf of the ISSVA board and scientific committee. Pediatrics 2015;136:203–14.

[7] Jones EW, Orkin M. Tufted angioma (angioblastoma). J Am Acad Dermatol 1989;20:214–25.

[8] Ji Y, Chen S, Xiang B, Li K, Xu Z, Yao W, et al. Sirolimus for the treatment of progressive kaposiform hemangioendothelioma: a multicenter retrospective study. Int J Cancer 2017;141:848–55.

[9] Weiss SW. Kaposiform hemangioendothelioma. In: Fletcher CDM, Bridge JA, Hogendoorn PCW, Mertens F, editors. WHO classification of tumours of soft tissue and bone. IARC: Lyon; 2013.

[10] Sahm F, Schrimpf D, Jones DT, Meyer J, Kratz A, Reuss D, et al. Next-generation sequencing in routine brain tumor diagnostics enable an integrated diagnosis and identifies actionable targets. Acta Neuropathol 2016;131:903–10.

[11] Ten Broek RW, Eijkelenboom A, van der Vleuten CJ, Kamping E, Kets M, Verhoeven BH, et al. Comprehensive molecular and clinicopathological analysis of vascular malformations: a study of 319 cases. Genes Chromosomes Cancer 2019;58:541–50.

[12] Lim YH, Bacchiocchi A, Qiu J, Straub R, Bruckner A, Bercovitch L, et al. Yale Center for mendelian genomics, McNiff J, Ko C, Robison-Bostom L, Antaya R, Halaban R, choate KA. GNA14 somatic mutation causes congenital and sporadic vascular tumors by MAPK activation. Am J Hum Genet 2016;99:443–50.

[13] Joseph NM, Brunt EM, Marginean C, Nalbantoglu I, Snover DC, Thung SN, et al. Frequent GNAQ and GNA14 mutations in hepatic small vessel neoplasm. Am J Surg Pathol 2018;42:1201–7.

[14] Bean GR, Joseph NM, Folpe AL, Horvai AE, Umetsu SE. Recurrent GNA14 mutations in anastomosing haemangiomas. Histopathology 2018;73:351–62.

[15] Barcley SF, Inman KW, Luks VL, McIntyre JB, Al-Ibraheemi A, Church AJ, et al. A somatic activating NRAS variant associated with kaposiform lymphangiomatosis. Genet Med 2019;21:1517–24.

[16] Croteau SE, Kozakewich HPW, Perez-Atayde AR, Fishman SJ, Alomari AI, Chaudry G, et al. Kaposiform lymphangiomatosis: a distinct aggressive lymphatic anomaly. J Pediatr 2014;164:383–8.

[17] Hoepfner KP, Karcher A, Shin DS, Craig L, Arthur LM, Carney JP, Tainer JA. Structural biology of RAD50 ATPase: ATP-driven conformational control in DNA double-strand break repair and the ABC-ATPase superfamily. Cell 200;101:789–800.

[18] Kinoshita E, van der Linden E, Sanchez H, Wyman C. RAD50, an SMC family member with multiple roles in DNA break repair: how does ATP affect function? Chromosome Res 2009;17:277–88.

[19] Rojowska A, Lammens K, Seifert FU, Direnberger C, Feldmann H, Hopfner KP. Structure of the RAD50 DNA double strand break repair protein in complex with DNA. EMBO J 2014;33:2847–59.

[20] Boscolo E, Limaye N, Huang L, Kang KT, Soblet J, Uebelhoer M, et al. Rapamycin improves TIE2-mutated venous malformation in a murine model and human subjects. J Clin Invest 2015;125:3491–504.

[21] Tirana P, Dore M, Cerezo VN, Cervantes M, Sanchez AV, Ferrereo MM, et al. Sirolimus in the treatment of vascular anomalies. Eur J Pediatr Surg 2017;27:86–90.

[22] Schmid I, Klenk AK, Sparber-Sauer M, Koscielniak E, Maxwell R, Häberle B. Kaposiform hemangioendothelioma in children: a benign vascular tumor with multiple treatment options. World J Pediatr 2018;14:322–9.